



## PAPER

# Reducing 4D CT imaging artifacts at the source: first experimental results from the respiratory adaptive computed tomography (REACT) system

RECEIVED  
5 September 2019REVISED  
5 February 2020ACCEPTED FOR PUBLICATION  
27 February 2020PUBLISHED  
8 April 2020Natasha Morton<sup>1</sup>, Jonathan Sykes<sup>2,3</sup>, Jeffrey Barber<sup>2,3</sup> , Christian Hofmann<sup>4</sup>, Paul Keall<sup>1</sup>  and Ricky O'Brien<sup>1</sup> <sup>1</sup> ACRF Image X Institute, Faculty of Medicine and Health, The University of Sydney, Australia<sup>2</sup> Blacktown Cancer and Haematology Centre, Sydney West Cancer Network, Blacktown Hospital, Australia<sup>3</sup> Institute of Medical Physics, School of Physics, The University of Sydney, Australia<sup>4</sup> Siemens AG, Imaging and Radiotherapy, Forchheim, GermanyE-mail: [nmor8420@uni.sydney.edu.au](mailto:nmor8420@uni.sydney.edu.au)

Keywords: prospective gating, motion artifacts, 4D CT

## Abstract

Breathing variations during 4D CT imaging often manifest as geometric irregularities known as respiratory-induced image artifacts and ultimately effect radiotherapy treatment efficacy. To reduce such image artifacts we developed Respiratory Adaptive Computed Tomography (REACT) to trigger CT acquisition during periods of regular breathing. For the first time, we integrate REACT with clinical hardware and hypothesize that REACT will reduce respiratory-induced image artifacts  $\geq 4$  mm compared to conventional 4D CT.

4D image sets were acquired using REACT and conventional 4D CT on a Siemens Somatom scanner. Scans were taken for 13 respiratory traces (12 patients) that were reproduced on a lung-motion phantom. Motion was observed by the Varian RPM system and sent to the REACT software where breathing irregularity was evaluated in real-time and used to trigger the imaging beam. REACT and conventional 4D CT images were compared to a ground truth static-phantom image and compared for absolute geometric differences within the region-of-interest. Breathing irregularity during imaging was retrospectively assessed using the root-mean-square error of the RPM measured respiratory signal during beam on (RMSE\_Beam\_on) for each phase of the respiratory cycle.

REACT significantly reduced the average frequency of respiratory-induced image artifacts  $\geq 4$  mm by 70% for the tumor ( $p = 0.003$ ) and 76% for the lung ( $p = 0.0002$ ) compared to conventional 4D CT. Volume reductions of 10% to 6% of the tumor and 2% to 1% of the lung compared to conventional 4D CT were seen. Breathing irregularity during imaging (RMSE\_Beam\_on) was significantly reduced by 27% ( $p = 0.013$ ) using the REACT method.

For the first time, REACT was successfully integrated with clinical hardware. Our findings support the hypothesis that REACT significantly reduced respiratory-induced image artifacts compared to conventional 4D CT. These experimental results provide compelling evidence for further REACT investigation, potentially providing clearer images for clinical use.

## 1. Introduction

Four Dimensional Computed Tomography (4D CT) provides a set of time-resolved 3D images spanning the entire breathing cycle (Vedam *et al* 2003). Since its development over 15 years ago, 4D CT has become a crucial tool for 4D radiotherapy and Stereotactic Body Radiotherapy (SBRT) planning for thoracic and upper abdominal cancer patients (Li *et al* 2008, Rosu and Hugo 2012). However, current 4D CT methods rely on patient breathing to remain constant throughout the imaging process and imaging parameters are selected based on the patient's initial respiratory pattern. Variations from this initial breathing pattern can

manifest in the resulting images as geometric inaccuracies, misalignments of anatomical boundaries and in extreme cases can obfuscate the tumor entirely. A study by Yamamoto *et al* (2008) found 90% of 50 patient 4DCT scans contained a respiratory-induced image artifact greater than 4 mm, where an artifact was defined as an anatomical misalignment between the image edge and the ‘true’ edge. These artifacts can propagate through the entire radiotherapy treatment process, notably, reducing clinician confidence in tumor volume delineation, negatively impacting image registration for patient set up, tumor tracking and dose accumulation, and introducing variations to the internal target volume (ITV) during treatment (Persson *et al* 2010, Szegedi *et al* 2012, Chan *et al* 2013, Yoganathan *et al* 2017). The detrimental effects of these artifacts are beginning to emerge in novel staging and functional imaging techniques such as ventilation imaging (Yamamoto *et al* 2013), PET/4D CT and radiomics (Yip and Aerts 2016, Du *et al* 2019, Tanaka *et al* 2019).

There have been a number of methods proposed to reduce respiratory-induced image artifacts in 4D CT including oversampling (Castillo *et al* 2015), successive quick scans (O’Connell *et al* 2018), data-driven post-image processing (Hertanto *et al* 2012, Hinkle *et al* 2012, Zhang *et al* 2013), retrospective trace analysis for localized rescanning (Werner *et al* 2019), patient guidance (Goossens *et al* 2014, Pollock *et al* 2016) and manual gating (Pan *et al* 2017). Despite the development of various methods, their wide spread implementation and adoption into the clinic has been limited by several factors including excessive dose, computation time, image registration errors, workload and operator variation.

Respiratory Adaptive Computed Tomography (REACT, formerly termed RMG4DCT in some simulation studies) is an automatic prospective-gating technique developed to reduce operator intervention and imaging dose, and to avoid acquisition during irregular patient respiration. By avoiding breathing changes, we aim to reduce respiratory-induced image artifacts that present as geometric irregularities, such as elongation or overlapping of the patient’s anatomy in the final 4D CT image set. The technique was first proposed in 2007 (Keall *et al* 2007) and has evolved through *in silico* studies to include adaptive gating regions based on both phase and displacement variations, allowing for real-time gating of the imaging machine (Langner and Keall 2010, Bernatowicz *et al* 2015, Martin *et al* 2018). REACT acquires images only when necessary, using all data in the final reconstruction, reducing imaging dose (> 20% reduction in *in silico* beam on time (Langner and Keall 2009)), and adapting to patient breathing variations to reduce beam on trace irregularity (50% reduction (Langner and Keall 2010)). Through an industry partnership, essential control of x-ray acquisition has been provided to enable experimental investigations, taking a step towards clinical translation. This paper represents the first implementation of a fully automated and real-time REACT system on clinical hardware. We hypothesize that REACT will decrease respiratory-induced image artifacts  $\geq 4$  mm as compared to conventional step-and-shoot 4D CT.

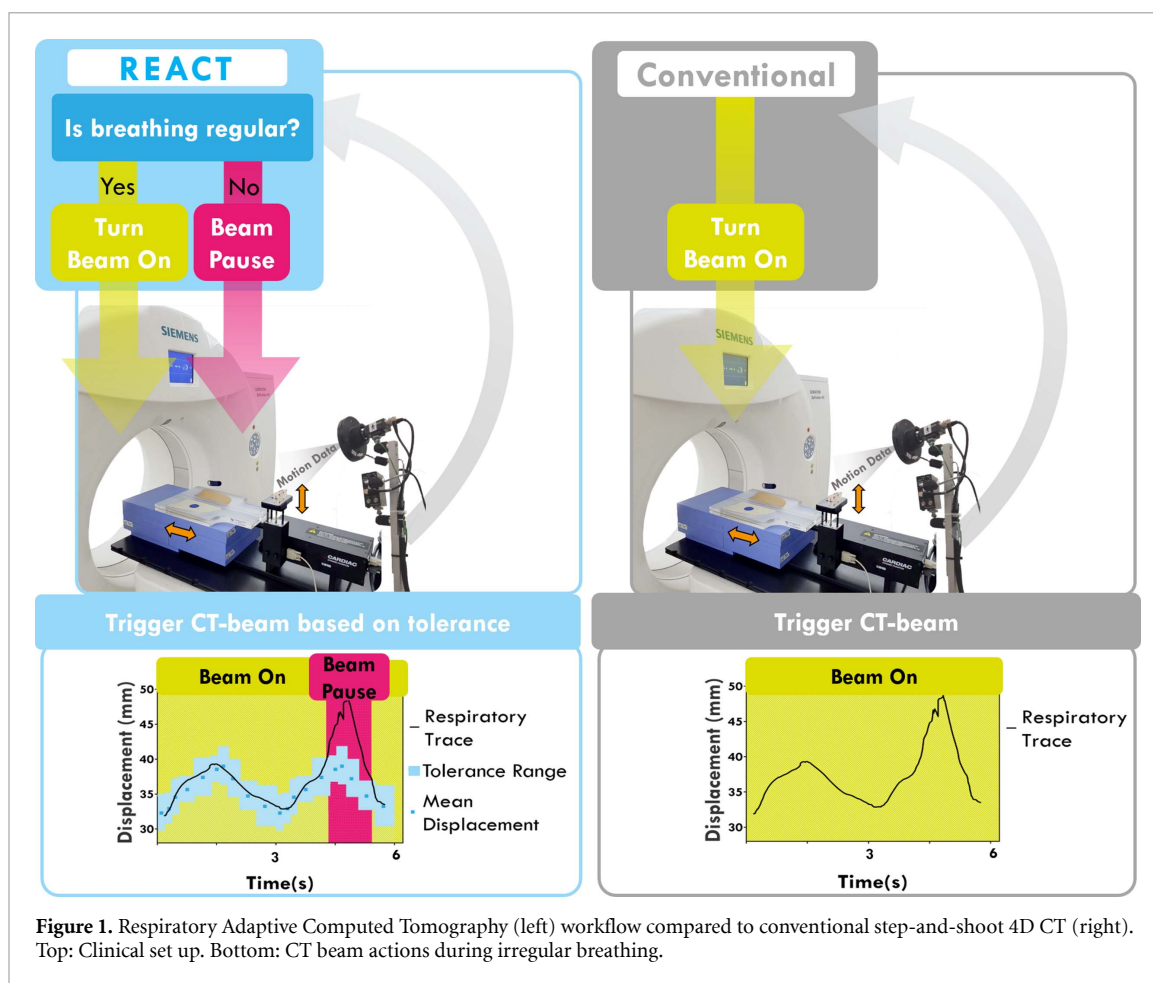
## 2. Materials and Method

### 2.1. REACT overview

The REACT system links the patient’s breathing signal to a fully automated C# software that triggers CT acquisitions based on real-time signal processing and analysis (see figure 1). The breathing signal can be imported from any tracking system that provides real-time displacement measurements. For the purposes of this paper, the Varian Real-time Position Management system (RPM) [Varian Medical Systems, Palo Alto CA] (Bernatowicz *et al* 2015) was chosen due to its widespread clinical use for conventional 4D CT imaging. In the software, the CT operator can specify several signal and scan settings such as the number of respiratory bins to acquire per breath (usually set to 10). Directly prior to imaging, the system undergoes a training period of 60 s to learn the patient’s average breathing rate, size and shape. These data are used to determine the displacement average  $\bar{d}_\theta$  and standard deviation  $\sigma_\theta$  for each respiratory phase bin  $\theta$  that will immediately be used to determine potential beam gating. The phase bins are equidistant in time between adjacent inhale peaks.

As the training period ends, imaging automatically commences. Throughout the entire imaging process the breathing displacement,  $d(t)$ , at time,  $t$ , is constantly monitored and the respiratory phase is calculated in real-time using the method proposed by Ruan *et al* (2009). The REACT system is connected to a Siemens Somatom Definition AS 64 slice CT scanner through the Open Interface Port and only acquires if the current breathing data point is within the displacement gating window for the current phase bin,  $\theta$ , i.e. if  $\bar{d}_\theta - \sigma_\theta \leq d(t) \leq \bar{d}_\theta + \sigma_\theta$ . However, if the patient’s breathing period or peak-to-peak displacement increases, as seen in figure 1 (bottom left), it shifts out of the gating window, displayed in blue and the system will respond by not triggering the CT beam, shown in pink. The system will continue to suppress acquisitions until the breathing data re-enters the gating window. This process continues until the end of the scan. A more detailed analysis of the displacement and phase gating window is given in (Martin *et al* 2018).

The REACT system is based on a ‘step-and-shoot’ or ‘cine’ 4D CT protocol. This means that the couch is stationary as imaging data is acquired. Once data spanning an entire breath are collected, the couch shifts to



the next position. Theoretically, for the REACT system, the patient can stay at one couch position indefinitely until their breathing re-enters the gating window and CT acquisition resumes. In practice, the maximum time spent at each couch position is limited by clinical throughput, patient compliance and CT machine ‘time out’ (which occurs after 30 s of inactivity on our clinical scanner). As a result, we have implemented an adaptive gating window: After 15 s, if no acquisition is made, the gating window increases by one standard deviation (e.g. to  $\bar{d}_0 - 2\sigma_0 \leq d(t) \leq \bar{d}_0 + 2\sigma_0$ ), and again after another 10 s of inactivity (e.g. to  $\bar{d}_0 - 3\sigma_0 \leq d(t) \leq \bar{d}_0 + 3\sigma_0$ ). After 30 s the scan will end (the upper limit on Siemens CT machines for beam time out). In a clinical setting, the decision to continue scanning would be made by the CT operator.

To accommodate hardware compatibility, a number of changes were made to the REACT software as compared to previous simulation studies. These changes include:

- Integration of external breathing signal from clinical respiratory monitoring devices.
- Integration of microcontroller to trigger CT beam acquisition and facilitate talk back from the scanner through the Open Interface Port. Discussed further in *Experimental Setup*.
- Adaptive gating windows with timing tailored to prevent CT inactivation time out after 30 s. Discussed further in *REACT Overview*.
- Additional options for one-phase acquisition compared to standard multi-phase acquisition to account for automatic couch translation. Discussed further in *REACT Imaging Protocol*.

## 2.2. Experimental implementation

To test the integration of the REACT system with the Varian RPM system and the Siemens Somatom Definition AS 64 slice scanner, we imaged a lung motion phantom with thirteen respiratory traces measured from 12 patients. To compare its efficacy in reducing respiratory-induced imaging artifacts, conventional step-and-shoot 4D CT scans were taken on the same phantom that reproduced the same respiratory traces. Respiratory-induced image artifacts were quantified in both the REACT and conventional image sets and compared (described in detail in the ‘Artifact Quantification’ section below).

**Table 1.** Metrics for first 3 min of thirteen respiratory traces across 12 patients systematically selected from the Virginia Commonwealth University tumor motion database.

Trace number (irregularity percentile)	Displacement RMSE (mm)	Mean peak to trough displacement $\pm$ standard deviation (mm)	Mean breath length $\pm$ standard deviation (s)
1 (5th)	0.24	12.8 $\pm$ 0.7	3 $\pm$ 0.2
2 (10th)	0.27	8.6 $\pm$ 0.5	4.9 $\pm$ 0.4
3 (20th)	0.33	7.7 $\pm$ 0.9	3.2 $\pm$ 0.2
4 (25th)	0.35	6.3 $\pm$ 1.2	2.9 $\pm$ 0.3
5 (30th)	0.39	21.6 $\pm$ 2	3.4 $\pm$ 0.4
6 (40th)	0.44	14.4 $\pm$ 2.1	2.7 $\pm$ 0.3
7 (50th)	0.50	8.9 $\pm$ 1.3	3.4 $\pm$ 0.4
8 (60th)	0.56	11.5 $\pm$ 1.2	3.2 $\pm$ 0.5
9 (70th)	0.62	5.3 $\pm$ 1.3	4.3 $\pm$ 0.8
10 (75th)	0.65	18.7 $\pm$ 3.3	3.8 $\pm$ 1.0
11 (80th)	0.69	5.5 $\pm$ 1.4	4.1 $\pm$ 0.9
12 (90th)	0.79	6.7 $\pm$ 1.4	2.9 $\pm$ 1.0
13 (95th)	0.85	8 $\pm$ 2.8	2.7 $\pm$ 1.0

### 2.2.1. Experimental setup

The phantom design was a combination of a CIRS Dynamic Thorax Phantom 008A motor (Computerized Imaging Reference Systems, Inc. Norfolk, VA) and a Standard Imaging IMRT phantom body (Standard Imaging, Inc. Middleton, WI) as shown in figure 1. The body consisted of an acrylic slab with air-equivalent lung and water-equivalent tumor insert with a 4 cm diameter. Patient-measured abdominal motion, discussed in the section below, was sent to the phantom via the CIRS Motion Control 2.5.8 software. The traces were rigidly mimicked by the phantom body in the superior-inferior direction and the chest motion surrogate in the anterior-posterior direction. The same data were used in both motion directions with a one-to-one correlation and were synchronously sent to the phantom via the CIRS motion control software.

Phantom motion was measured by detecting the displacement changes of a reflective marker block placed on the chest motion surrogate. This signal was sent to the REACT computer through a COM port connected to the RPM computer in the CT control room. The REACT software made decisions on the breathing regularity, as specified in the section above. If the motion was within the displacement tolerance, a digital pulse was sent to the CT machine through the Open Interface Port via a microcontroller. Once this signal was received by the CT, the beam was triggered and imaging data (CT slice) was acquired for one gantry rotation. The beam then paused and waited for the next signal. This process continued until the end of the scan.

### 2.2.2. Patient trace selection

A set of free-breathing motion traces were taken from the Virginia Commonwealth University breathing training database (Hugo *et al* 2016). 1D anterior-posterior (AP) chest motion under free breathing conditions was acquired using the Varian RPM system during a previous audio-visual biofeedback study (110 free breathing traces from 24 patients) and during fluoroscopic kilovoltage imaging for a lung tumor motion study (523 free breathing traces from 31 patients), totaling 633 breathing traces across 55 patients (George *et al* 2006, Hugo *et al* 2017). In accordance with the AAPM report for Task Group 76 on managing respiratory motion in radiation oncology (Keall *et al* 2006), motion management is recommended for traces with an average peak-to-trough displacement greater than 5 mm. As such, traces with peak-to-trough displacement less than this threshold were excluded from the data set, leaving 596 traces.

In order to assess the remaining traces for breathing variability, including changes in breath shape, baseline drift and amplitude, the displacement root mean square error (RMSE) was used and is defined in equation 1. The RMSE was calculated for the first three minutes of each patient trace and determines the displacement variation from the mean for every phase of the breathing cycle (each phase being 1 degree of 360 degrees). The traces were ordered by the measure of trace irregularity, from which the 5th, 10th, 20th, 25th, 30th, 40th, 50th, 60th, 70th, 75th, 80th, 90th and 95th percentile traces were chosen for this experiment to represent a range of patient respiratory motion shown in table 1.

$$\text{RMSE} = \sqrt{\frac{\sum_{i=1}^M \sum_{\emptyset=1}^N (d_{i,\emptyset} - \bar{d}_{\emptyset})^2}{N \times M}} \quad (1)$$

Here represents a displacement data point from the respiratory motion trace with index  $i = \{1, 2, \dots, M\}$  (where  $M =$  total data points per phase). Each data point is assigned a phase value of  $\emptyset = \{1, 2, \dots, N\}$

(where  $N = 360$ ) dependent on its location between peak-inhale points. The root mean squared difference is taken between each displacement data point  $d_{i,\theta}$  and the average displacement across all data points with phase value  $\theta$ .

### 2.2.3. React Imaging protocol

A thoracic prospective-gating protocol, which allows for set displacement gating of one respiratory bin in a step-and-shoot setting, was used. This proved to have limitations for testing REACT experimentally: After every externally triggered acquisition, the CT couch fed 17 mm to the next position. Ideally, the CT couch would feed to the next position after 10 externally triggered acquisitions (one for each respiratory phase).

To account for this hardware limitation, four separate scans were taken for each respiratory trace, each acquiring for a different respiratory bin. This was achieved by accounting for all 10 respiratory bins within the REACT software, as though taking an entire REACT 4D CT, but only sending a signal to trigger the CT beam for the one selected phase. The breathing phase was divided into ten evenly-spaced phase bins where four, sampling respiratory motion at displacement extremes and mid-values, were chosen for acquisition and reconstruction.

The scan settings were set as: 0.36 s gantry rotation time, 17 mm couch feed, 2 mm slices. Image reconstruction was achieved using Siemens Syngo software with a 500 mm reconstruction diameter, 2 mm slices and a B30 f medium kernel.

### 2.2.4. Conventional Imaging Protocol

Our scanner did not have a step-and-shoot 4D CT protocol, so conventional step-and-shoot 4D CT had to be acquired in a similar manner to the above section, that is, one respiratory bin per scan with the scans repeated four times for each of the four respiratory phase bins. Conventional methods vary with manufacturer and are dependent on a number of factors involving reconstruction methods and hardware specifications. For the purposes of this paper, the conventional step-and-shoot 4D CT method described by Pan (2005) was simulated. Due to the automatic couch feed, a number of constraints were put in place to ensure the described conventional method was appropriately replicated, such as:

- (a) Maximum couch stay time was defined as the average breath length plus one second. Only one acquisition could be made within this time frame. The extra second allows for small changes in the patient's breathing period, ensuring enough data are collected for image reconstruction.
- (b) The Varian RPM real-time calculated phase was used to determine when to acquire.
- (c) If no acquisition was made within the maximum couch stay time (due to an increased breath length), an acquisition was forced. The couch position was noted and the corresponding slice was discarded post reconstruction and replaced with the neighboring slice.

It is important to note that on some scanners the breathing trace can be retrospectively viewed and the points of peak-inhale can be modified prior to reconstruction. This was not possible in this study.

The scan and image reconstruction settings were consistent with REACT and noted in the above section.

### 2.2.5. Artifact Quantification

To aid in quantifying the number of respiratory-induced image artifacts in both the REACT and conventional scans, a static phantom ground truth image was taken.

The tumor and the lung in each image (REACT, Conventional and ground truth) was individually segmented into a binary region of interest using Otsu's method for global intensity thresholding (Otsu 1979). The average tumor and lung position during acquisition was calculated from the recorded RPM motion trace and used to rigidly register each region of interest to the static phantom ground truth. The ground truth static image was subtracted from each moving (REACT and conventional 4D CT) image. If a value difference in corresponding pixels was found, it was assigned a value of 1, if no difference was found it was assigned a value of 0, resulting in a binary difference map as shown in figure 2. This map shows geometric variations in the region of interest shape and size as compared to the ground truth.

Each difference map was assessed, slice by slice in the sagittal direction, for pixels with a value of 1. If any pixels were found, this was recorded and considered a respiratory-induced image artifact. The number of superiorly or inferiorly adjacent pixels with the same value were counted and considered the magnitude of the respiratory-induced image artifact. In figure 2 for example, there are two artifacts within the same sagittal slice: Artifact 1, with a magnitude of four pixels (8 mm), and Artifact 2, with a magnitude of two pixels (4 mm). 4 mm was used as a lower threshold to compare respiratory-induced image artifacts between the two acquisition methods using a one-tailed Wilcoxon Signed Rank Test across all traces ( $N = 13$ ). This was

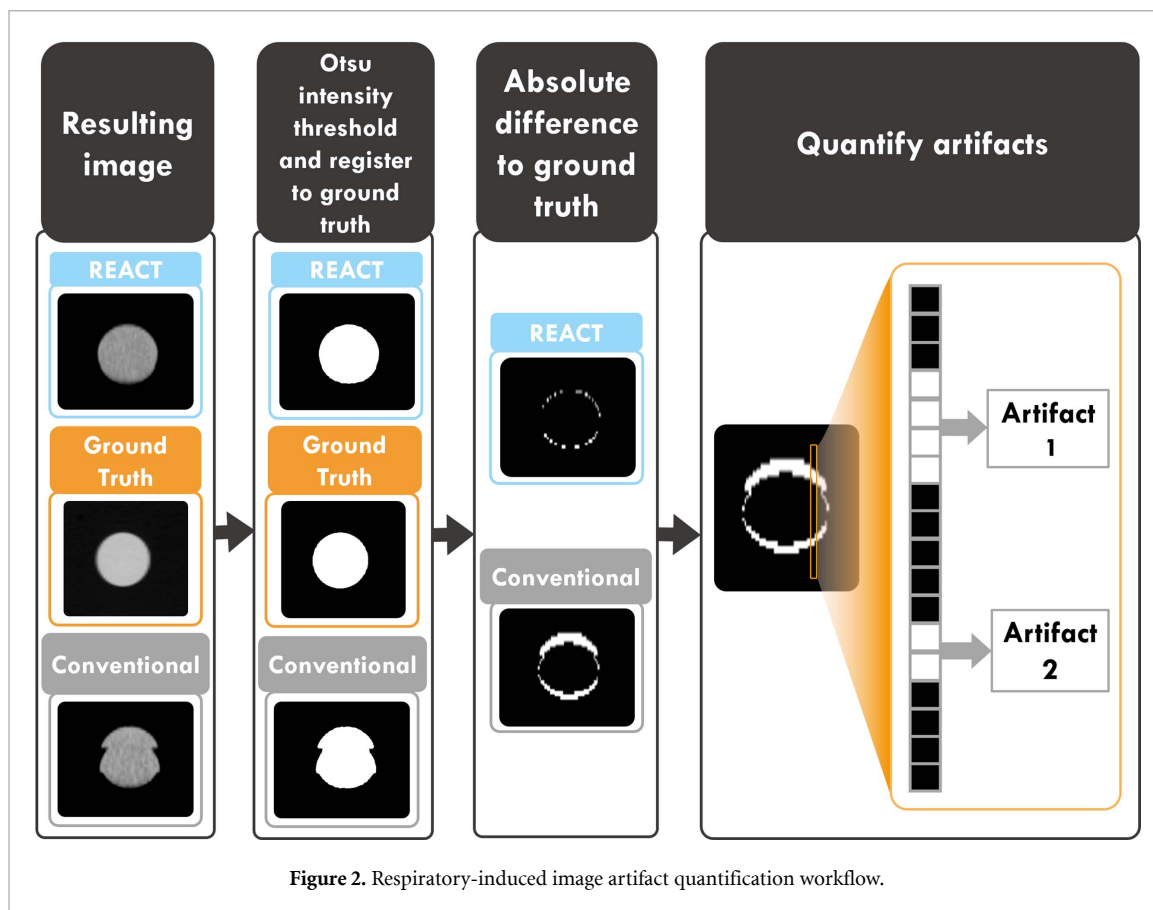


Figure 2. Respiratory-induced image artifact quantification workflow.

deemed a lower limit of respiratory-induced image artifact detection using human observers in Yamamoto *et al* (2008).

The numbers of respiratory-induced image artifacts ( $> 0$  mm) for both the tumor and lung were also multiplied by the transverse pixel size in order to determine the absolute change in volume as a percentage of the ground truth.

#### 2.2.6. Breathing Irregularity during Imaging

x-ray acquisition was logged in real-time for each data point by the REACT software during the scan process. Breathing displacement during image acquisition was retrospectively assessed for all 13 breathing traces across both REACT and conventional 4D CT and used to determine breathing irregularity. The breathing irregularity was quantified using the RMSE\_Beam\_on as specified in equation 1. A one-tailed Wilcoxon Signed Rank test was used to determine whether REACT reduced trace irregularity during imaging compared to conventional 4D CT.

#### 2.2.7. Latencies

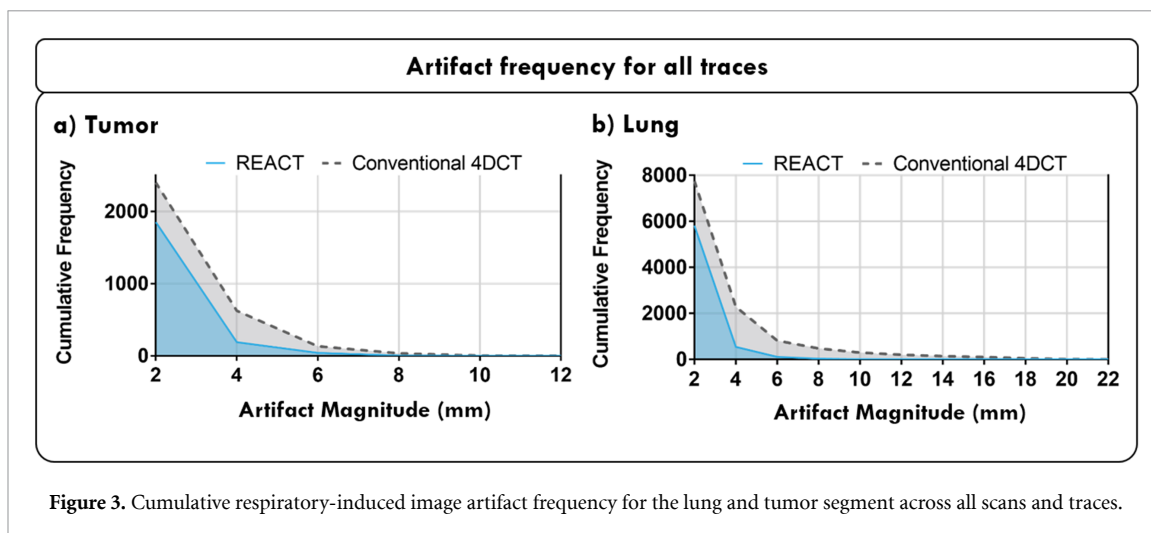
The Varian RPM system passed motion data at 25 Hz (40 ms) to the REACT software where the main decision loop from the received data point to an acquisition decision has been measured at  $< 1$  ms on average. The delay between consecutive acquisitions was 505 ms.

The time from the sent acquisition signal (from REACT software) to the received x-ray on signal (from the scanner) was quantified by comparing the time a trigger signal sent from the REACT software to the time it received a beam on signal from the scanner.

## 3. Results

### 3.1. Respiratory-induced image artifact reduction for each trace

Overall, REACT significantly reduced the average frequency of respiratory-induced image artifacts  $\geq 4$  mm by 70% for the tumor ( $p = 0.003$ ) and 76% for the lung ( $p = 0.0002$ ) compared to conventional step-and-shoot 4D CT, see figure 3. The reduction in artifact-affected area was reduced from 10% to 6% of the tumor and 2% to 1% of the lung compared to conventional 4D CT. The reduction in respiratory-induced image artifacts supports the hypothesis that REACT reduces respiratory-induced image artifacts  $\geq 4$  mm



compared to conventional step-and-shoot 4D CT. The results for all respiratory-induced image artifact magnitudes can be found in figure 3 below.

For the tumor region, REACT reduced respiratory-induced image artifacts  $\geq 4$  mm by  $\geq 70\%$  for 10 traces, 28% for one trace and introduced artifacts in the 10th ( $-18\%$ ) and 25th ( $-200\%$ ) percentile traces. The greatest reduction (100%) was seen for the 20th and 80th percentile traces. The former had the least number of respiratory-induced image artifacts (only 1  $> 4$  mm) and the latter experienced both displacement and breath length variations that were effectively gated for. For the lung region, REACT decreased respiratory-induced image artifacts  $\geq 4$  mm by  $> 50\%$  for all traces, with 10 reduced by  $> 70\%$ . The greatest reduction (95%) was seen for the 60th percentile trace which experienced considerable baseline variations, images for which can be found in figure 4. The reduction of respiratory-induced image artifacts  $\geq 4$  mm for each trace can be found in figure 5.

### 3.2. Respiratory-induced image artifact reduction for each respiratory phase

The smallest reduction in artifacts was seen for the peak-inhale phase with 77% reduction in artifacts  $\geq 4$  mm for the tumor region and 72% for the lung region (figure 6). The greatest reduction of 95% for the lung region was seen for the peak-exhale phase. The greatest reduction of 95% for the tumor was seen in the mid exhale phase and can be seen in figure 6.

### 3.3. Breathing Irregularity during Imaging

The mean RMSE\_Beam\_on was significantly reduced by 27.3% ( $p = 0.013$ ) from 1.12 mm for conventional 4D CT to 0.82 mm for REACT. The largest reduction of 2.23 mm was seen for the 90th percentile trace where an isolated 2 cm displacement variation was avoided during imaging using REACT. All but two REACT traces had a reduced RMSE\_Beam\_on value compared to conventional 4D CT. The exceptions were the 30th percentile trace ( $-0.39$  mm reduction) and the 70th percentile trace ( $-0.08$  mm reduction).

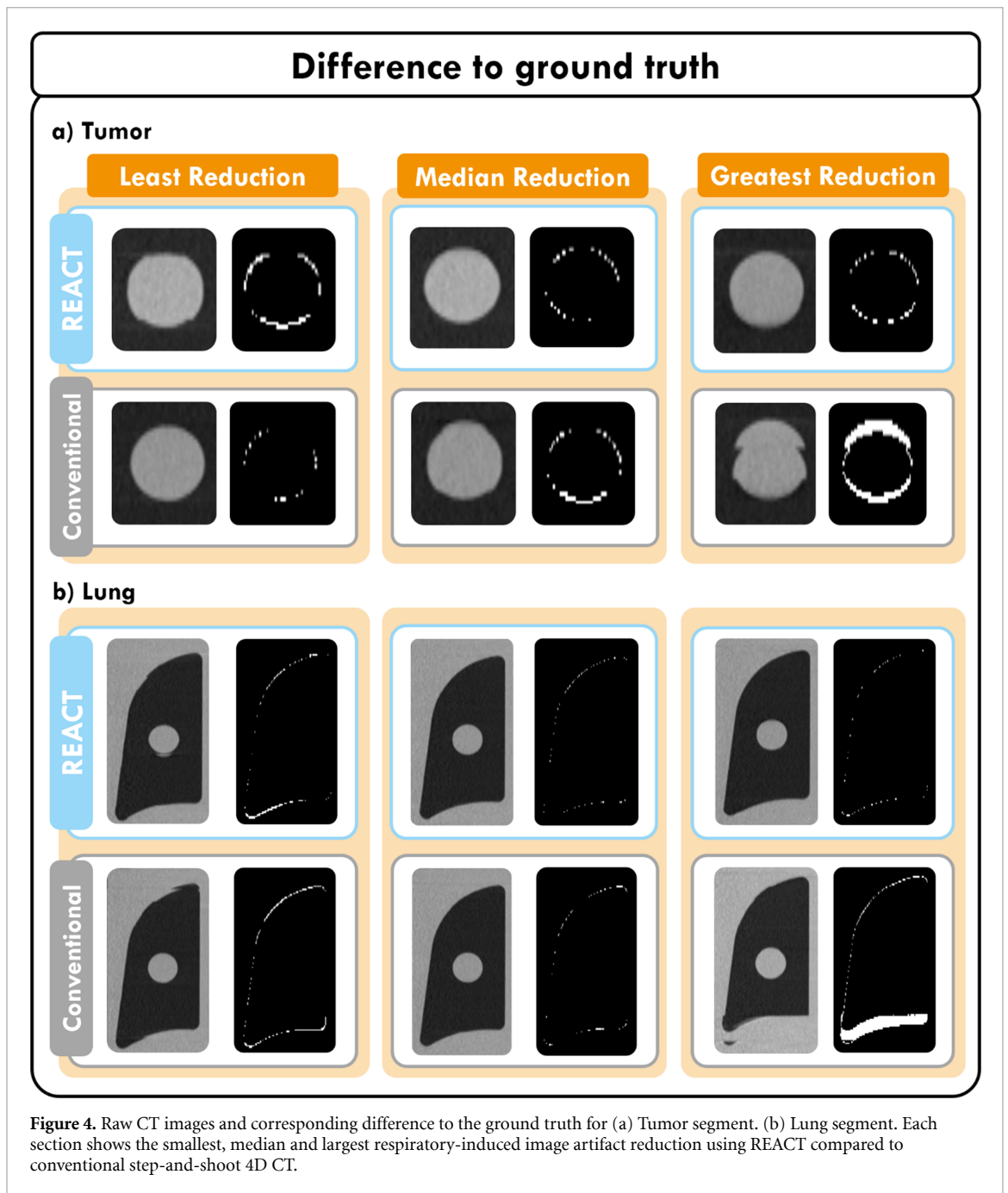
### 3.4. Latencies

The delay between sending a beam on signal and actual beam on was found to be 11 ms on average with a maximum delay of 18 ms.

## 4. Discussion

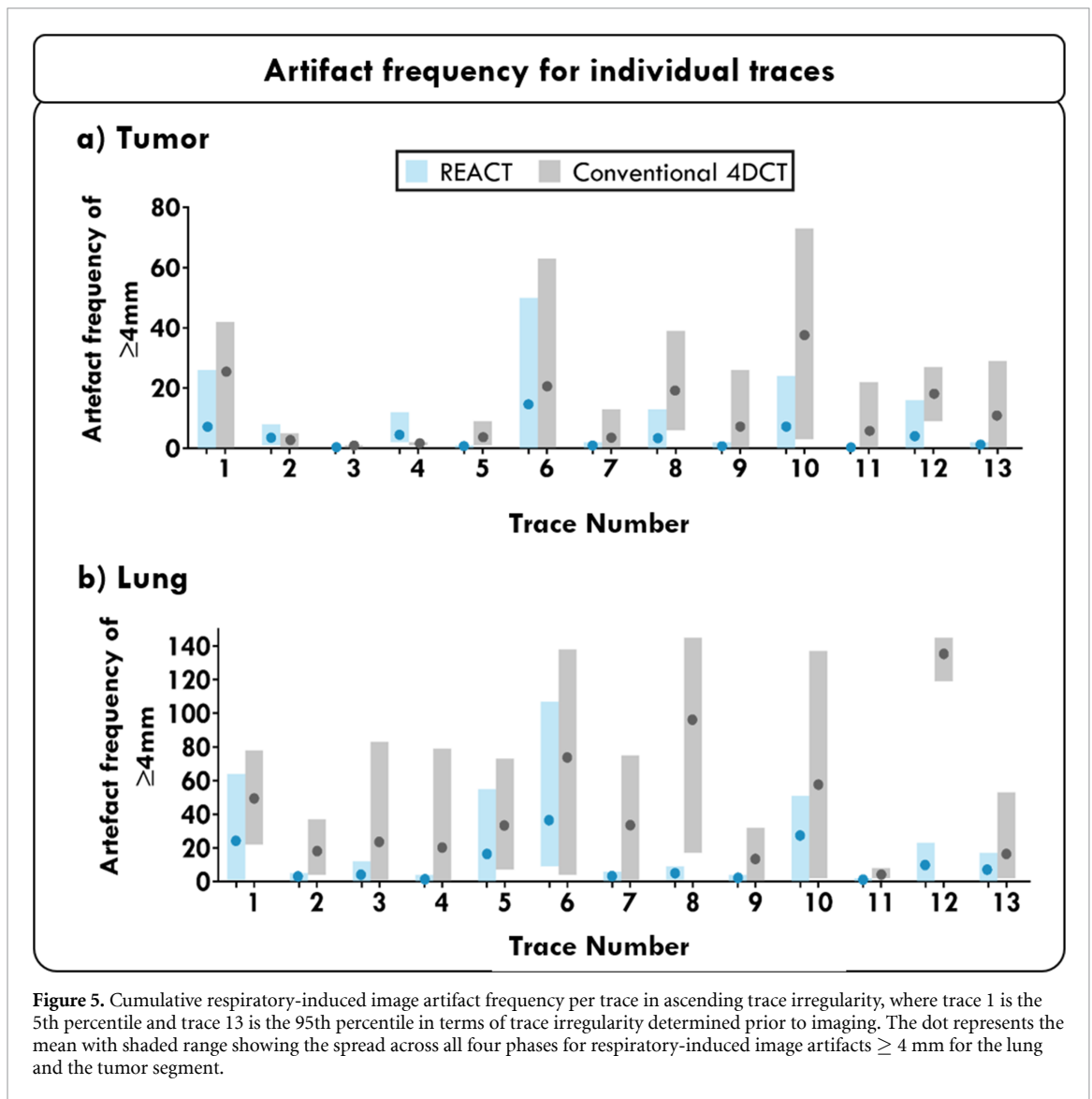
In this study we have integrated REACT on clinical hardware for the first time. We have quantified and compared respiratory-induced image artifacts present in both REACT and conventional step-and-shoot 4D CT scans for thirteen patient traces. The results support the hypothesis that REACT significantly reduces respiratory-induced image artifacts  $\geq 4$  mm compared to conventional 4D CT.

Overall, the reduction of respiratory-induced image artifacts using REACT was clear and this was seen throughout all scans in the lung region. Ten of the thirteen traces exhibited a reduction in the tumor region  $> 70\%$  using REACT with two of the remaining traces resulting in an increase in respiratory-induced image artifacts. After investigation it was found that the real-time phase estimation used in REACT was susceptible to perturbations in the RPM displacement signal caused during couch feed. The REACT phase estimation was required to readjust, leading to acquisition lags sometimes large enough to cause misalignments of a few



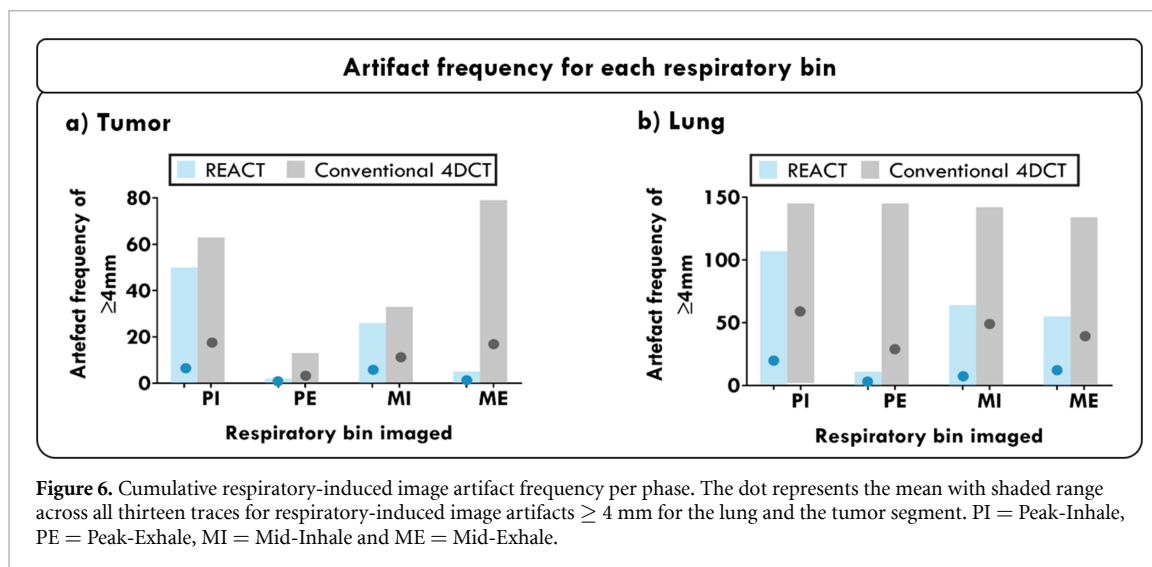
mm between slices. While this proved an issue for two traces, the remaining traces were unaffected. The breathing traces used in this study were recorded using an RPM device on real lung cancer patients during CBCT imaging. As a result, realistic patient motion while lying on a table is inherently included in the phantom motion and additional noise added by the RPM is simply a result of the RPM mount setup.

The peak-exhale phase exhibited the least number of respiratory-induced image artifacts overall, but the greatest reduction in artifacts, where there was a 75% reduction in the tumor region and a 95% reduction in the lung region using REACT. Peak-exhale is of importance in motion modeling due to its relative stability compared to other phases of the respiratory cycle, a notion substantiated in this study. Motion-modeling techniques, whether for synthesizing 4D CT images at set respiratory phases or for gating or tracking during treatment delivery, rely heavily on the initial 4D CT image set (McClelland *et al* 2013, Fassi *et al* 2014). For example, a number of motion models require deformation vector fields obtained from registering each 4D CT phase to a base image, often the peak-exhale phase (Zhang *et al* 2013). For synthesizing artifact-free images, the motion model is then reapplied to the base image (Hertanto *et al* 2012). It is evident that respiratory-induced image artifacts can still be present in the peak-exhale phase and REACT's ability to reduce these artifacts may result in superior performance over conventional 4D CT for motion modeling and reduces the need for image synthesis.



While the overall reduction in respiratory induced image artifacts from REACT is evident, it is important to note that the conventional 4D CT scans were not reconstructed based on retrospectively adjusted peak-inhale tags. While this is clinical routine for retrospective 4D CT protocols, the prospective-gating protocol required in this study did not allow for immediate retrospective analysis prior to reconstruction. To quantify the impact of this limitation, a comparison between the RPM-defined peaks (used for acquisition and reconstruction in this study) and the inhale peaks as retrospectively determined from the displacement data, was made. An average offset between the detected peaks was 0.185 s, which, for the fastest breathing trace used in this study (2.7 s average breath length), falls within the length of one phase bin. It should also be noted that the number of respiratory-induced image artifacts present in the conventional 4D CT scans did not correlate with the irregularity metric used to determine respiratory traces for the study. As the scan time for each trace could not be known prior to imaging, the RMSE was determined based on the first three minutes of data for each trace. In most cases, the scans took less than three minutes, where irregularities that occurred outside of the scanning time frame (i.e. towards the end of the trace or during the training period) could not contribute towards image artifacts. Additionally, the RMSE metric provides an average measure of irregularity favoring changes in amplitude, however, respiratory-induced image artifacts are often caused from large, isolated breathing variations such as a patient coughing. Traces 1 and 6 show a large number of artifacts for a breathing trace with a relatively low RMSE. Although these traces experienced a relatively repeatable signal, the breathing amplitude was large with a fast breathing rate leading to large tumor motion within the acquisition window.

A key challenge of any motion study is accurately replicating complex patient motion. In an ideal setting, a deformable and anatomically correct phantom would be used to properly characterize artifact reduction, accounting for a motion gradient from the upper lung to the diaphragm as well as hysteresis. Unfortunately, to the best of our knowledge, such a phantom does not exist. As such, a rigid motion was applied to a simple



lung phantom with a chest surrogate using a one-to-one correlation between tumor and surrogate (chest) motion. Clinically, the correlation between tumor motion and the external respiratory signal can vary, likely leading to an increase in respiratory-induced image artifacts. Currently, both conventional 4D CT and REACT cannot correct for these artifacts. As such, this study focuses on irregularities in the measured breathing signal, which we believe to be the leading cause of image artifacts. Datamining has the potential to provide the information required to detect changing conditions in the internal-external respiratory correlation and could be used to adapt the REACT gating thresholds in future versions. It is important to note, therefore, that while the artifacts seen across the lung and tumor in this study are simple in nature, the same setup and motion conditions were applied to both REACT and conventional 4D CT scans allowing for quantitative analysis of respiratory-induced artifact reduction.

The forced couch feed after a single image acquisition in step-and-shoot mode presented as a large limitation to the study, preventing the acquisition of multiple CT phases in one scan. The time required to image all ten respiratory phases in this manner would not be clinically viable compared to conventional 4D CT. This hardware limitation cannot be overcome without significant changes to the CT scanner and as such, vendor participation. For certain scanners, such as the one used in this study, helical acquisition is the only option for 4D CT imaging. While it results in faster scan times, the continuous couch motion and complex reconstruction makes implementing and analyzing REACT in helical mode a challenging task.

In the current setup there are some aspects that we believe will differ from a full (10 phase) REACT scan. In this study, respiratory-induced image artifacts were decreased by  $\sim 70\%$  and breathing irregularity during acquisition by 27.3%. Previous studies found a decrease in respiratory-induced image artifacts of  $\sim 50\%$  and breathing irregularity during acquisition of 11.8%. The reason for this difference is two-fold. First, this study looks at four of ten reconstructed phase bins compared to ten in previous studies. As the number of phase bins per scan increases, as does the chance data points will fall outside of the gating window for regular breathing. Any expansion of the gating window will then accept a greater range of breathing variation, limiting the impact of artifact reduction. Second, the gating window in this study expands by one standard deviation rather than doubling in size as implemented in (Martin *et al* 2018). In this manner, large irregularities are gated for while keeping the total scan time down. As a result, we would expect a full ten phase REACT scan to deliver a decrease in image respiratory-induced image artifacts somewhere between the current value and previous simulation studies.

Compared to conventional 4D CT, previous simulation studies of REACT saw the scan time double on average (Langner and Keall 2010, Bernatowicz *et al* 2015, Martin *et al* 2018) and we expect a complete ten phase REACT scan to follow a similar trend. One advantage of REACT, seen in this study, is that it can account for changes in breathing frequency. This is unlike conventional step-and-shoot 4D CT that must wait for the maximum couch stay time before shifting to the next position. Regardless, we still expect an increase in scan times over the conventional 4D CT method. In a previous simulation study accounting for all ten phase bins, Martin proposed an adaptive gating window that doubled in size after ten breaths of no acquisition (Martin *et al* 2018), this is a 40 s wait for a patient with an average breath of 4 s potentially adding minutes to the scan time for some patients. In this study we have implemented an adaptive gating window that increases by a smaller degree and at a faster rate than Martin (15 s of no acquisition), minimizing the increase in scan time. The potential to acquire multiple respiratory phases within one acquisition could be realized in future studies to aid in reducing the scan time further.

It is important to note that although REACT may increase the overall scan time, it affords a reduction in beam on time, and by extension, imaging dose. The limitations imposed on this study prevented a meaningful assessment of beam on time. In principle, the conventional step-and-shoot 4D CT simulated in this paper acquires imaging data for the entire time spent at each couch position. Only a subset of data is then used for image reconstruction, resulting in unnecessary dose. For example, a scan with an average breath length of 4 s, requiring ten respiratory bins would result in 12 acquisitions at minimum (20% wasted data) (Pan 2013), although it should be noted that some scanners and reconstruction methods share data across bins (thus reducing wasted dose). REACT keeps track of each acquisition in real-time and the corresponding respiratory bin. For the above example, REACT would lead to 10 acquisitions at every couch position, resulting in 0% wasted data. From this standpoint, REACT would be an ideal choice over artifact reducing methods such as oversampling, that increase the number of acquisitions even further, to account for an increase in breath length.

Baseline drift can be a large issue in the clinic, leading to an increase in respiratory-induced image artifacts that are not always obvious to the eye and can therefore result in poor ITV estimation; this is a problem in current clinical practice as well as for REACT. To our knowledge, baseline drift is not routinely accounted for in the clinic during conventional 4D CT scanning, and rescanning or repositioning is only made at the discretion of the CT operator or medical physicist post-scan. The gating window implemented in this study is adaptive, allowing the system to not only account for small variations in breathing shape but also in breathing baseline. If a baseline drift is great enough, the trace will move out of the gating window for an extended period, halting the scan. This allows for changes to be made, similar to current clinical practice, and the CT operator can choose to restart the scan from the beginning or continue scanning from the current couch position. In this study, all scans were completed and did not time out due to baseline changes. For future work we will add the option to either stop the scan as done in this study or to continue imaging the remaining field of view without the gating region, as per standard 4D CT.

In this study, we have integrated a new prospectively gated 4D CT technique on existing clinical hardware, where the only additional equipment is a computer to run the REACT software and a simple microcontroller to allow external triggering of the CT beam. Its similarity to the current 4D CT approach in set up, acquisition and reconstruction allows for easy adoption into the clinical work flow, yet, hardware limitations, such as the automatic couch feed, will need to be overcome before REACT can replace conventional 4DCT methods in the clinic.

## 5. Conclusion

REACT has been experimentally realized, providing fully automated and real-time adaptive image acquisition on a clinical CT scanner. Compared to a conventional 4D CT method, REACT successfully reduced respiratory-induced image artifacts, supporting our hypothesis, for thirteen patient modeled breathing traces across four key breathing phases. With further integration, REACT provides a distinct pathway to clearer images for clinical use.

## Acknowledgments

J Sykes and J Barber acknowledge the support of the NSW Department of Health. P Keall and R O'Brien are supported by an NHMRC Senior Principal Research Fellowship and a Cancer Institute NSW Career Development Fellowship, respectively.

The authors acknowledge the technical and funding support from Siemens Healthineers and graphical support from the ACRF Image X Institute Design and Communication officer, Julia Johnson.

## Conflicts of Interest

The authors would like to present the following conflicts of interest: C Hofmann is an employee of Siemens. P Keall is an inventor on a patent related to the research subject. P Keall and R O'Brien are investigators on a research agreement between Siemens and the University of Sydney.

## ORCID iDs

Jeffrey Barber  <https://orcid.org/0000-0003-0233-0970>

Paul Keall  <https://orcid.org/0000-0003-4803-6507>

Ricky O'Brien  <https://orcid.org/0000-0002-6586-7356>

## References

- Bernatowicz K, Keall P, Mishra P, Knopf A, Lomax A and Kipritidis J 2015 Quantifying the impact of respiratory-gated 4D CT acquisition on thoracic image quality: a digital phantom study *Med. Phys.* **42** 324–34
- Castillo S J, Castillo R, Castillo E, Pan T, Ibbott G, Balter P, Hobbs B and Guerrero T 2015 Evaluation of 4D CT acquisition methods designed to reduce artifacts *J. Appl. Clin. Med. Phys.* **16** 4949
- Chan M K, Kwong D L, Ng S C, Tong A S and Tam E K 2013 Experimental evaluations of the accuracy of 3D and 4D planning in robotic tracking stereotactic body radiotherapy for lung cancers *Med. Phys.* **40** 041712
- Du Q et al 2019 Radiomic feature stability across 4D respiratory phases and its impact on lung tumor prognosis prediction *PLoS One* **14** e0216480
- Fassi A, Schaerer J, Fernandes M, Riboldi M, Sarrut D and Baroni G 2014 Tumor tracking method based on a deformable 4D CT breathing motion model driven by an external surface surrogate *Int. J. Radiat. Oncol. Biol. Phys.* **88** 182–8
- George R, Chung T D, Vedam S S, Ramakrishnan V, Mohan R, Weiss E and Keall P J 2006 Audio-visual biofeedback for respiratory-gated radiotherapy: impact of audio instruction and audio-visual biofeedback on respiratory-gated radiotherapy *Int. J. Radiat. Oncol. Biol. Phys.* **65** 924–33
- Goossens S, Senny F, Lee J A, Janssens G and Geets X 2014 Assessment of tumor motion reproducibility with audio-visual coaching through successive 4D CT sessions *J. Appl. Clin. Med. Phys.* **15** 47–56
- Hertanto A, Zhang Q, Hu Y C, Dzyubak O, Rimner A and Mageras G S 2012 Reduction of irregular breathing artifacts in respiration-correlated CT images using a respiratory motion model *Med. Phys.* **39** 3070–9
- Hinkle J, Szegedi M, Wang B, Salter B and Joshi S 2012 4D CT image reconstruction with diffeomorphic motion model *Med. Image Anal.* **16** 1307–16
- Hugo G D, Weiss E, Sleeman W C, Balik S, Keall P J, Lu J and Williamson J F 2017 A longitudinal four-dimensional computed tomography and cone beam computed tomography dataset for image-guided radiation therapy research in lung cancer *Med. Phys.* **44** 762–71
- Hugo G D, Weiss E, Sleeman W C, Balik S, Keall P J, Lu J and Williamson J F 2016 Data from 4D lung imaging of NSCLC patients The Cancer Imaging Archive
- Keall P J et al 2006 The management of respiratory motion in radiation oncology report of AAPM Task Group 76 *Med. Phys.* **33** 3874–900
- Keall P J, Vedam S S, George R and Williamson J F 2007 Respiratory regularity gated 4D CT acquisition: concepts and proof of principle *Australas Phys. Eng. Sci. Med.* **30** 211–20
- Langner U W and Keall P J 2009 Accuracy in the localization of thoracic and abdominal tumors using respiratory displacement, velocity, and phase *Med. Phys.* **36** 386–93
- Langner U W and Keall P J 2010 Quantification of artifact reduction with real-time cine four-dimensional computed tomography acquisition methods *Int. J. Radiat. Oncol. Biol. Phys.* **76** 1242–50
- Li G, Citrin D, Camphausen K, Mueller B, Burman C, Mychalczak B, Miller R W and Song Y 2008 Advances in 4D medical imaging and 4D radiation therapy *Technol. Cancer Res. Treat.* **7** 67–81
- Martin S, O'Brien R, Hofmann C, Keall P and Kipritidis J 2018 An in silico performance characterization of respiratory motion guided 4DCT for high-quality low-dose lung cancer imaging *Phys. Med. Biol.* **63** 155012
- McClelland J R, Hawkes D J, Schaeffter T and King A P 2013 Respiratory motion models: a review *Med. Image Anal.* **17** 19–42
- O'Connell D, Ruan D, Thomas D H, Dou T H, Lewis J H, Santhanam A, Lee P and Low D A 2018 A prospective gating method to acquire a diverse set of free-breathing CT images for model-based 4DCT *Phys. Med. Biol.* **63** 04NT03
- Otsu N 1979 A threshold selection method from gray-level histograms *IEEE Trans. Syst. Man Cybern.* **9** 62–6
- Pan T 2005 Comparison of helical and cine acquisitions for 4D-CT imaging with multislice CT *Med. Phys.* **32** 627–34
- Pan T 2013 Helical 4D CT and comparison with cine 4D CT *4D Modeling and Estimation of Respiratory Motion for Radiation Therapy* ch 2 (Berlin: Springer) pp 25–41
- Pan T, Martin R M and Luo D 2017 New prospective 4D-CT for mitigating the effects of irregular respiratory motion *Phys. Med. Biol.* **62** N350–61
- Persson G E, Nygaard D E, Brink C, Jahn J W, Munck A F, Rosenschold P, Specht L and Korreman S S 2010 Deviations in delineated GTV caused by artefacts in 4DCT *Radiother. Oncol.* **96** 61–6
- Pollock S, Kipritidis J, Lee D, Bernatowicz K and Keall P 2016 The impact of breathing guidance and prospective gating during thoracic 4DCT imaging: an XCAT study utilizing lung cancer patient motion *Phys. Med. Biol.* **61** 6485–501
- Rosu M and Hugo G D 2012 Advances in 4D radiation therapy for managing respiration: part II - 4D treatment planning *Z. Med. Phys.* **22** 272–80
- Ruan D, Fessler J A, Balter J M and Keall P J 2009 Real-time profiling of respiratory motion: baseline drift, frequency variation and fundamental pattern change *Phys. Med. Biol.* **54** 4777–92
- Szegedi M, Sarkar V, Rassiah-Szegedi P, Wang B, Huang Y J, Zhao H and Salter B 2012 4D CT image acquisition errors in SBRT of liver identified using correlation *J. Appl. Clin. Med. Phys.* **13** 164–73
- Tanaka S, Kadoya N, Kajikawa T, Matsuda S, Dobashi S, Takeda K and Jingu K 2019 Investigation of thoracic four-dimensional CT-based dimension reduction technique for extracting the robust radiomic features *Phys. Med.* **58** 141–8
- Vedam S S, Keall P J, Kini V R, Mostafavi H, Shukla H P and Mohan R 2003 Acquiring a four-dimensional computed tomography dataset using an external respiratory signal *Phys. Med. Biol.* **48** 45–62
- Werner R, Sentker T, Madesta F, Gauer T and Hofmann C 2019 Intelligent 4D CT sequence scanning (i4DCT): concept and performance evaluation *Med. Phys.* **46** 3462–74
- Yamamoto T, Kabus S, Lorenz C, Johnston E, Maxim P G, Diehn M, Eclon N, Barquero C, Loo B W Jr. and Keall P J 2013 4D CT lung ventilation images are affected by the 4D CT sorting method *Med. Phys.* **40** 101907
- Yamamoto T, Langner U, Loo B W Jr., Shen J and Keall P J 2008 Retrospective analysis of artifacts in four-dimensional CT images of 50 abdominal and thoracic radiotherapy patients *Int. J. Radiat. Oncol. Biol. Phys.* **72** 1250–8
- Yip S S and Aerts H J 2016 Applications and limitations of radiomics *Phys. Med. Biol.* **61** R150–66
- Yoganathan S A, Maria Das K J, Subramanian V S, Raj D G, Agarwal A and Kumar S 2017 Investigating different computed tomography techniques for internal target volume definition *J. Cancer Res. Ther.* **13** 994–9
- Zhang Y, Yang J, Zhang L, Court L E, Balter P A and Dong L 2013 Modeling respiratory motion for reducing motion artifacts in 4D CT images *Med. Phys.* **40** 041716